International Journal of ChemTech Research
CODEN (USA): IJCRGG ISSN: 0974-4290
Vol.8, No.4, pp 1678-1688, 2015

Growth and characterization of nonlinear optical L- threonine cadmium chloride single crystal by Sankaranarayanan–Ramasamy (SR) method

K. Parasuraman[1], B. Milton Boaz[2]*

[1]Department of Physics, Sri Muthukumaran Institute of Technology, Chennai-600 069, India
[2]PG and Research Department of Physics, Presidency College, Chennai-600 005, India

Abstract: The bulk single crystal of L- threonine cadmium chloride (LTCC), an efficient semiorganic Non Linear Optical (NLO) material of size 60 mm in length, 15 mm in diameter, was grown successfully in unidirectional by Sankaranarayanan Ramasamy (SR) method. Single crystal X-ray diffraction study reveals that LTCC crystallizes into orthorhombic system with the space group $P2_12_12_1$. The unidirectional growth along the plane (2 0 2) was confirmed from the powder XRD pattern with the sharp peak having maximum intensity. Optical transmission spectrum shows that LTCC has highly transparent in the entire visible region with a wide band gap of 3.75 eV for large photon absorption. The Vicker's microhardness test is used for the assessment of fracture toughness, brittleness index and yield strength for the synthesized crystal. Dielectric constant and dielectric loss were calculated by varying frequencies at different temperatures. Photoluminescence study establishes that LTCC exhibit red emission in the wavelength region 615 nm. The laser induced surface damage threshold for the grown crystal was measured as 3.12 GW/cm^2 and SHG efficiency of the crystal is also examined by Kurtz's powder test using Nd: YAG Laser.
Keywords: Growth from solutions, Optical properties, Optical constant, Mechanical Properties.

1. Introduction

The development of highly efficient nonlinear optical materials for optoelectronic applications such as high speed information processing, optical communications and optical data storage has been the subject of intense research activity throughout the world, over the past two decades [1–3]. The synthesis of novel and efficient frequency conversion materials has resulted in the development of semi-organic materials, which possess large nonlinearity, high resistance to laser induced damage, low angular sensitivity and good mechanical stability [4–6]. In semi- organic materials, the organic ligand is ionically bonded with inorganic host. Due to this, the new semi-organic crystals have higher mechanical strength and chemical stability [7]. In recent years, considerable research efforts have been made in exploring novel semi-organic materials for their potential use in a variety of devices. From the stand-point of the search for newer nonlinear optical materials, amino acids offer a rich choice. Many optically active amino acids show highly efficient optical second harmonic generation (SHG) and are promising candidates for coherent blue– green laser generation and frequency doubling applications [8]. Complexes of amino acid with inorganic salts are promising materials for SHG property as they have the tendency to combine the advantage of the organic amino acid with the inorganic salt. Hence, L-arginine, L-histidine, L-threonium, L-alanine and L-valine have been subjugated for the formation of salts with different inorganic acids. As a result, very good semiorganic materials such as L-arginine phosphate monohydrate [9], L-histidine hydrochloride [10], L-valine hydrochloride [11], L-analine

cadmium chloride [12], L-analine zinc chloride [13], L-analine lithium chloride [14], L- threonine cadmium chloride [15] have been explored as the suitable materials for NLO applications. However, the information of bulk growth of LTCC for second harmonic generation devices is sketchy.

Hence, in the present work attempts are made to grow LTCC in bulk form by unidirectional growth using Sankaranarayanan Ramasamy (SR) method. High quality crystals of size 60 mm in length, 15 mm in diameter have been grown successfully with in a period of 23 days. The grown crystal is subjected to single crystal XRD, powder XRD, UV–visible transmission spectral analysis, microhardness measurement, dielectric characterization, laser damage threshold, photoluminescence spectral analysis. The NLO property of the crystal is also investigated by performing Kurtz powder test.

2. Experimental procedure

2.1. Synthesis

The title compound (LTCC) was synthesized by mixing purified L- threonine and cadmium chloride in de-ionized water in the stoichiometric ratio1:1. The reaction of synthesis process follows the equation,

$$C_4H_9NO_3 + CdCl_2 \longrightarrow Cd(C_4H_9NO_3)Cl_2 \quad (1)$$

2.2. Solubility studies

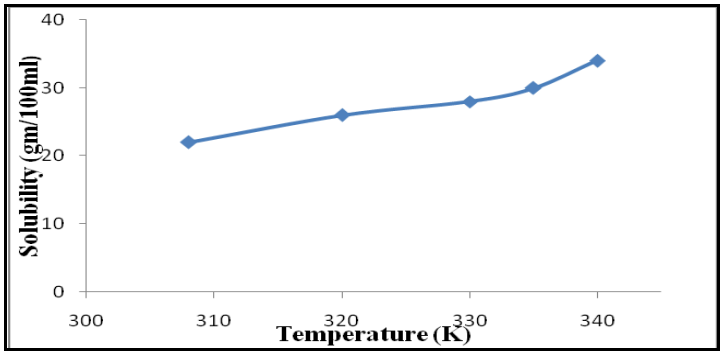

Fig. 1 Solubility curve of LTCC single crystal

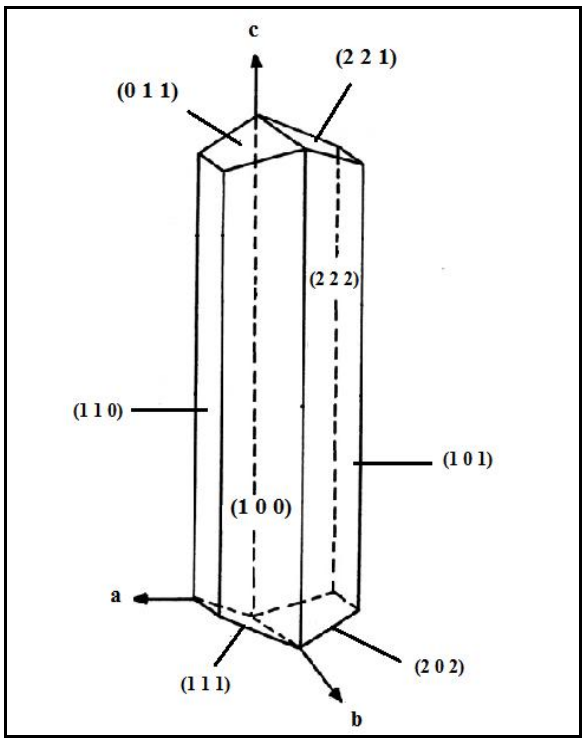

Fig. 2 Morphology of LTCC single crystal

Solubility of the material is a useful analysis to grow bulk single crystals from solution. The solubility of the synthesized salt was carried out using deionized water as solvent by gravimetric analysis [16] in the temperature range from 308 to 340 k. The solubility curve obtained for LTCC is shown in Fig.1. From the curve, it is observed that the material has positive solubility gradient with a solubility of 22 g/100 ml at 308 K. The Saturated solution prepared in accordance with the solubility data was allowed for slow evaporation at 308 K for obtaining the seed crystals. From the single crystal analysis, the morphology pattern of LTCC was generated and is depicted in Fig. 2. Out of the well known plane observed in the morphology pattern (2 0 2 plane along the direction (b-axis) has faster growth, good mechanical strength and physical property as compared to other planes. Hence, it is desirable to conduct the growth experiment in the favorable orientation (2 0 2) plane by keeping the polished seed and mounted at the bottom of the ampoule.

2.3. Growth assembly and crystal growth

The growth of good quality and large size NLO crystals with orientation control is needed for device application. The recently discovered Sankaranarayanan–Ramasamy (SR) [17] method is suitable to control the orientation during bulk crystal growth from solution. Based on the morphology of the LTCC crystal, the defect free clean surface (2 0 2) face was selected in the present study to impose the unidirectional growth. The SR method experimental set-up already reported [17-20] consists of a heating coil, thermometer, inner container, temperature controller, growth vessel and ampoule. A ring heater positioned at the top of the growth ampoule facilitated the solvent evaporation. The assembly was designed in such a way to obtain a maximum temperature profile at the top. An optically transparent seed was fixed at the bottom of the ampoule with (2 0 2) plane at the top and filled with the saturated solution of L-arginine and 4-nitrophenol. The ampoule was mounted along the axis of the inner cylinder. The ampoule was designed with an inner L-bend, which controls spontaneous nucleation on the top wall of the ampoule. Thus, the growth is initiated from the seed fixed at the bottom of the ampoule with desired orientation. The temperature of the top and bottom portion was set as 39 ˚ C and 35˚ C, respectively for the growing crystals. The temperature around the growth region is maintained at ±0.05 ˚C accuracy. The solvent is evaporated with respect to the temperature of the top portion. After few days, the seed crystal of LTCC mounted at the bottom starts to grow along the plane (2 0 2). Under this condition the highly transparent crystal was monitored and the growth system was kept constant for a long period for attaining continuous growth, which yields LTCC crystal of 74 mm length and 18 mm diameter within a period of 19 days. The photograph of the as grown crystal is shown in Fig. 3**.**

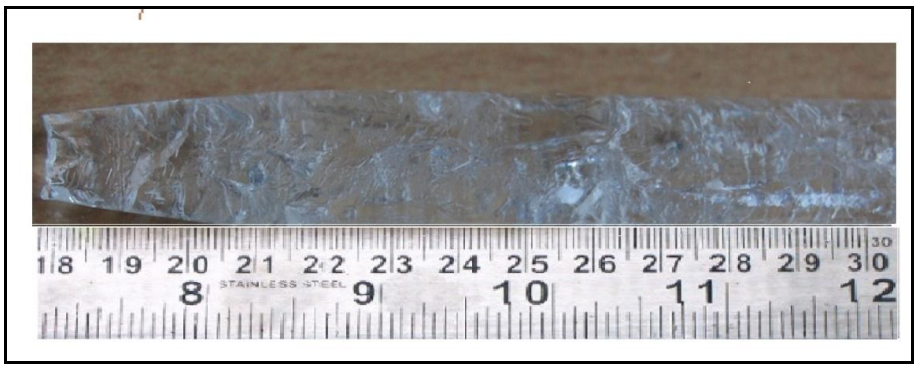

Fig. 3 Photograph of SR grown LTCC crystal

3. Results and discussion

3.1. Single crystal X-ray diffraction

The grown LTCC crystal is subjected to single crystal X-ray diffraction studies using Bruker Kappa APEX-2 diffractometer with Mo Kα (λ=0.71073 E) radiation to determine the cell parameters and crystal structure. The result of the study reveals that LTCC crystallizes into orthorhombic system with the space group $P2_12_12_1$. The lattice parameters obtained in the present study a=15.792 Å, b=5.822 Å and c=7.02 Å are in good agreement with the reported values [15].

3.2 Powder X-ray diffraction studies

Powder X-ray diffraction study was also carried out on the sample by Rich Seifert diffractometer using Cu Kα (λ=1.5418 Å) radiation. The powdered sample was scanned over the range of 2Θ values (10-70°) at a

scan rate of 2° per minute. The indexed X-ray diffraction pattern obtained for LTCC is shown in Fig. 4. The well defined sharp peaks on the pattern confirm that crystallites are properly oriented without any defects. It is also pertained to note that the peak corresponding to (2 0 2) has the maximum intensity in the pattern, which evinces that the crystal is growing unidirectional axis.

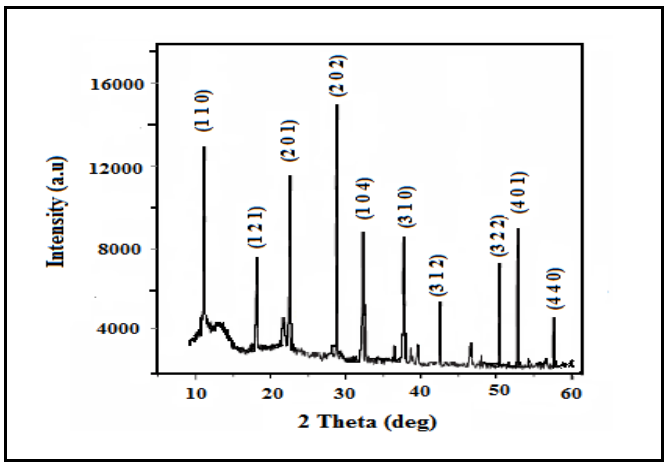

Fig. 4 Powder XRD pattern of LTCC crystal

3.3 optical transmission spectral studies

The optical transmission spectra of LTCC, single crystal was recorded in the region 200-2000 nm using the VARIAN CARRY 5E MODEL spectrometer covering the entire UV–vis and near infrared region. The recorded spectrum shown in Fig. 5, it is observed that the crystal possesses more than 80% transmission in the entire visible and near infrared region with the lower cut-off wavelength at 350 nm. This suggests that the material is quite suitable for SHG generation, UV tunable Laser and optoelectronic applications. The good transmission of the crystal in the entire visible region is important for NLO devices [21].

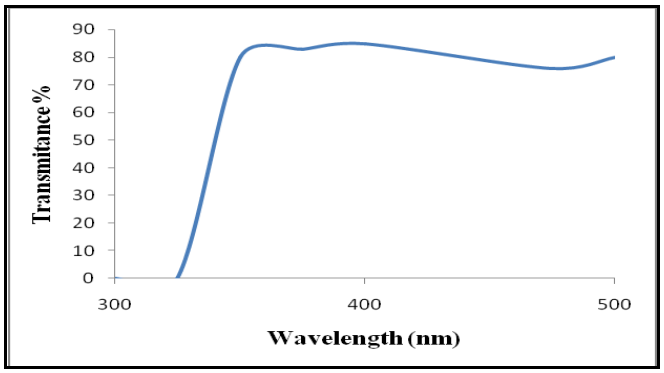

Fig. 5 Optical transmission spectrum of LTCC crystal

3.4. Determination of optical band gap

The dependence of optical absorption coefficient on photon energy helps to study the band structure and the type of transition of electrons. The optical absorption coefficient (α) was calculated from the transmittance spectra using the relation,

$$\alpha = \frac{2.3036\log(1/T)}{d} \qquad (2)$$

Where, T is the transmittance and d is the thickness of the crystal.

As a consequence direct band gap, the crystal under study has absorption co-efficient (α) obeying the relation for high photon energies (hν)

$$\alpha = \frac{A(h\nu - E_g)^{1/2}}{h\nu} \quad (3)$$

Where E_g is the band gap and A is a constant. The optical band gap of LTCC single crystal evaluated by extrapolating the linear portion of the plot between $(\alpha h\nu)^2$ and $(h\nu)$ is depicted in Fig. 6**.** The band gap calculated is found to be E_g = 3.75 eV. As a consequence of wide band gap, the grown crystal has large transmittance in the entire visible region [22].

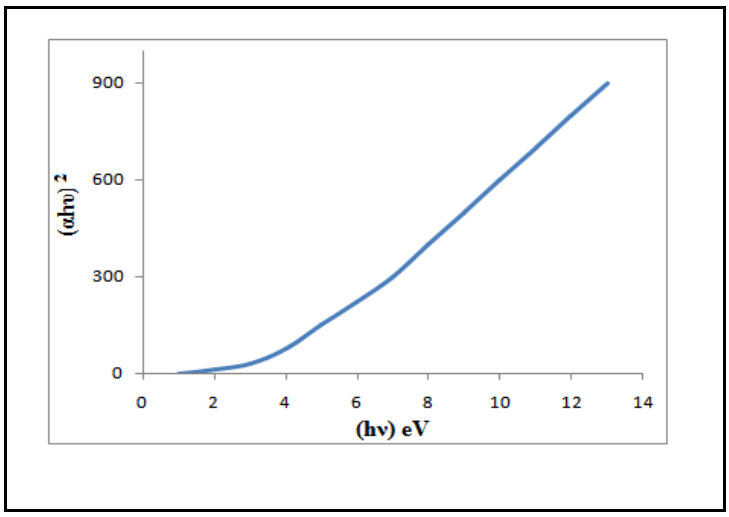

Fig. 6 Plot of α versus photon energy for LTCC crystal

3.5. Determination of optical constant

Optical behavior of materials is important to determine its usage in optoelectronic devices [23]. Knowledge of optical constant of a material such as optical band gap and extinction coefficient is quite essential to examine the material's potential optoelectronic applications [24]. Further, the optical properties may also be closely related to the material's atomic structure, electronic band structure and electrical properties.

The dependence of optical absorption co-efficient with photon energy helps to study the band structure and the type of transition of the electron. The absorption coefficient (α) and the optical constant (n, k) are determined from the transmission (T) and reflection (R) spectrum based on the following relations, [25,26]

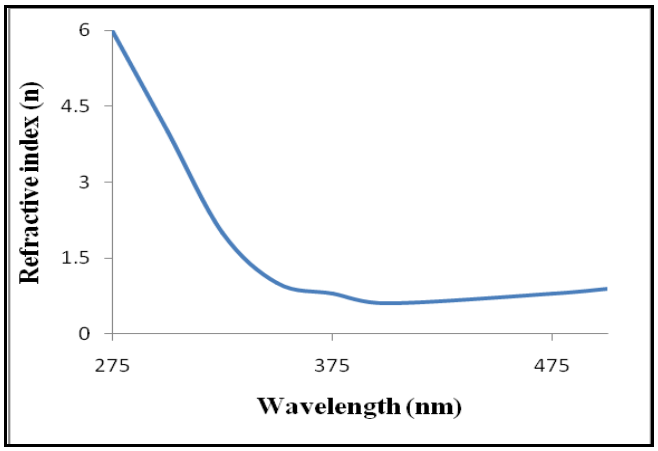

Fig.7.variation of refractive index with wavelength for LTCC crystal

$$T = \frac{(1-R)^2 \exp(-\alpha t)}{1 - R(-2\alpha t)} \quad (4)$$

The reflectance in terms of absorption coefficient can be calculated using the following relation [27]

$$R = 1 \pm \frac{\sqrt{1 - \exp(-\alpha t) + \exp(\alpha t)}}{1 + \exp(-\alpha t)} \quad (5)$$

and from the above equation the refractive index n, can be derived as

$$n = \frac{-\left(R + 1 \pm \sqrt{-3R^2 + 10R - 3}\right)}{2\,(R - 1)} \quad (6)$$

The dependence of refractive index (n) on wavelength is shown in Fig. 7.

3.6. Vickers microhardness test

The hardness of the material depends on different parameters such as, lattice energy, Debye temperature, heat of formation and interatomic spacing. The cut and well polished crystal was subjected to static indentation test at room temperature using Vicker's microhardness tester. Indentations were made on the sample plane with the load ranging from 50 to 200 g, by keeping the time of indentation constant at (10s) for all trials. The distance between the consecutive indentations were kept more than five times the diagonal length of the indentation, to avoid surface effects. The Vicker's hardness number (*Hv*) for different loads were calculated [28] using the relation.

$$Hv = 1.8544 \frac{p}{d^2} kg/mm^2 \quad (7)$$

Where, P is the applied load in kilogram, and d is the diagonal length of indentation impression in millimeter and 1.854 is a constant of a geometrical factor for the diamond pyramid. The variation of microhardness profile with applied load is shown in Fig. 8. From the profile it is observed that hardness increases with increasing load up to 102 g with maximum hardness number of 85 kg/mm^2. Further, the variation of load indicates that, above 102 g the hardness number decreases with increasing load. The decrease in hardness number with increase load provides information about the formation of cracks due to release of internal stress generated by local indentation. From the results, it is also concluded that the crystal has reverse indentation size effect due to increasing hardness number with respect load [29]. The work hardening coefficient n, which is measure strength of the crystal, is computed from the slope of log p versus log d plot (Fig. 9) is found to be 1.45.

According to Meyer's relation, P is related to d and n as

$$P = K_1 d^n \quad (8)$$

Where K_1 is the standard hardness value, which can be estimated from the plot of P versus d^n depicted Fig.10. Since, the material takes some time to revert to the elastic mode after every indentation, a correction x is applied to the d value and the Kick's law is written as,

$$P = K_2 (d + x)^2 \quad (9)$$

Simplifying equation (5) and (6) ,

$$d^{n/2} = \left(\frac{K_2}{K}\right)^{\frac{1}{2}} d + \left(\frac{K_2}{K_1}\right) x \quad (10)$$

The slope of $d^{n/2}$ versus d yields $\left(\frac{K_2}{K_1}\right)^{\frac{1}{2}}$ and the intercept is a measure of x as estimated from Fig. 11 .Also the fracture toughness (K_C) is given by,

$$K_C = \frac{P}{\beta c^{\frac{3}{2}}} \quad (11)$$

Where c is the crack length measured from the centre of the indentation mark to the crack tip, P is the applied load and β = 7 is the geometrical constant for Vickers' indenter. The brittleness index (B) is given by the formula,

$$B = \frac{H_V}{K_C} \quad (12)$$

From H_V and n the, yield strength σ_v of the material can be found out using the relation,

$$\sigma_v = \frac{H_V}{2.9}\{1-(2-n)\}\left[\frac{12.5(2-n)}{1-(2-n)}\right]^{2-n} \quad (13)$$

The load dependent hardness parameters calculated for LTCC crystal are presented in Table 1.

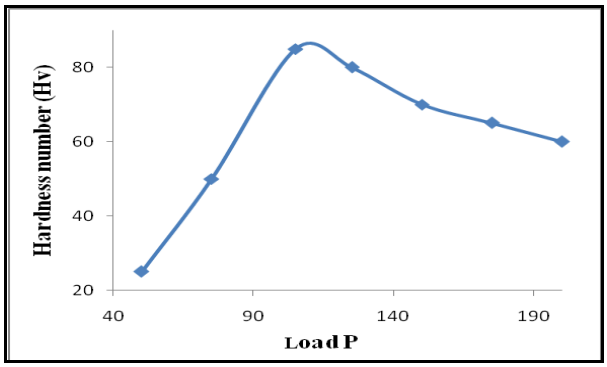

Fig .8 Plot of P versus Hv for LTCC crystal

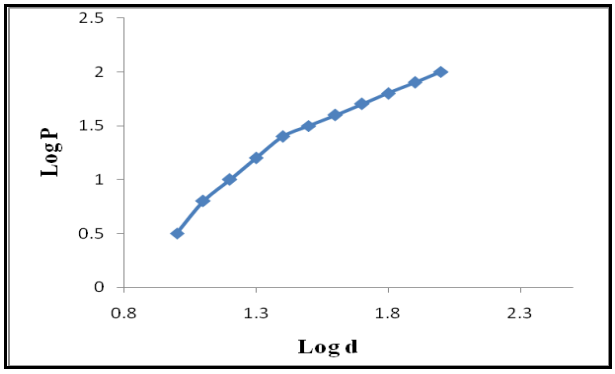

Fig. 9 Plot of log p versus log d for LTCC crystal

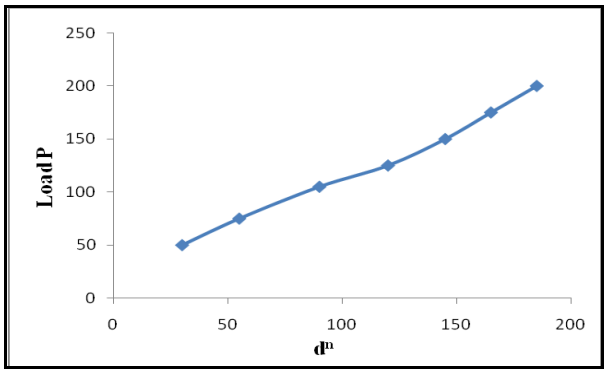

Fig. 10 Plot of d^n versus Load P for LTCC crystal.

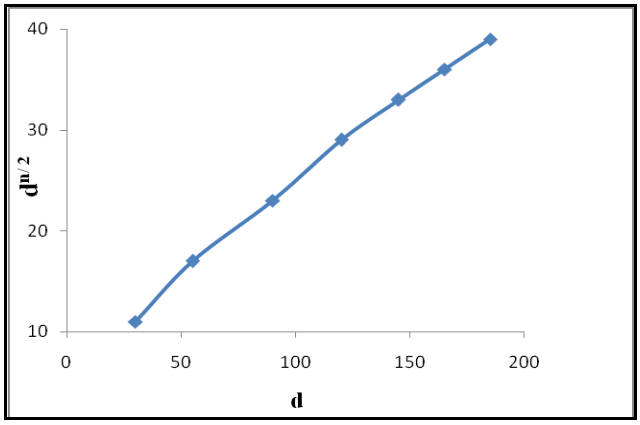

Fig. 11 Plot of $d^{n/2}$versus d for LTCC crystal.

Table 1 Micro hardness data obtained on the LAL crystal

Parameter	values
n	**1.45**
K_1 (kg/mm)	**22.45 x 10^{-2}**
K_2 (kg/mm)	**6.25 x 10^{-2}**
K_c ($MNm^{-3/2}$)	**0.0215**
B ($m^{-1/2}$)	**4.47x10^3**
σ_v(Mpa)	**124.25**

3.7. Dielectric studies

The Dielectric measurements for LTCC single crystal is carried out using HIOKI 3532-50 LCR HITESTER in the frequency range 50 Hz to 5 MHz for different temperatures. The selected sample is cut using a diamond saw and polished using paraffin oil and fine-grade alumina powder to obtain a good surface finish. Silver paste is coated on both side of the sample to increase the ohmic contact. The dielectric constant ε is calculated using the relation

$$\varepsilon = \frac{cd}{A\varepsilon_0} \qquad (14)$$

Where c is the capacitance, d is the thickness; *A* is the area of cross section and ε_0 is the absolute permittivity of the free space having the value 8.854x10^{-12} F/m. The dielectric loss ε' is also calculated using the relation,

$$\varepsilon' = \varepsilon \tan\delta \qquad (15)$$

The variation of dielectric constant and dielectric loss with frequency are shown in Fig.12 and 13 respectively. It is observed from the profile that both the dielectric constant and dielectric loss decrease with increase in frequency at room temperature**.** In general, the dielectric study provides information regarding the dielectric constant arises from the contribution of different polarizations mechanism, namely electronic, ionic, atomic, space charge, etc., developed in the material subjected to the electric field variations. The large dielectric constant at low frequency indicates the present of space charge polarization [30] arising at the grain boundary interface. The low value of dielectric loss at high frequencies reveal the high optical quality of the crystal with lesser defects, and this parameter is of vital importance for nonlinear optical applications [31].

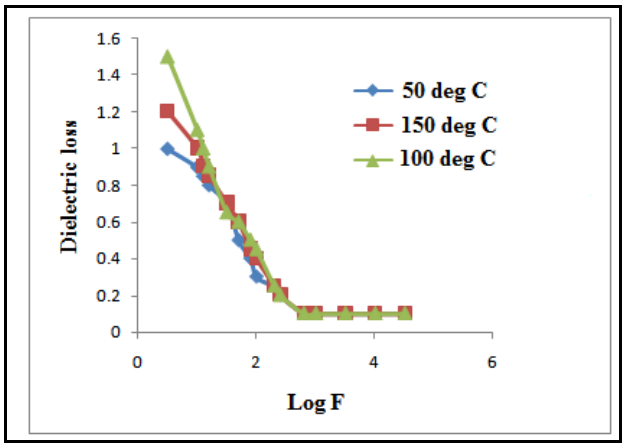

Fig. 12 Variation of dielectric constant with log f of LTCC crystal

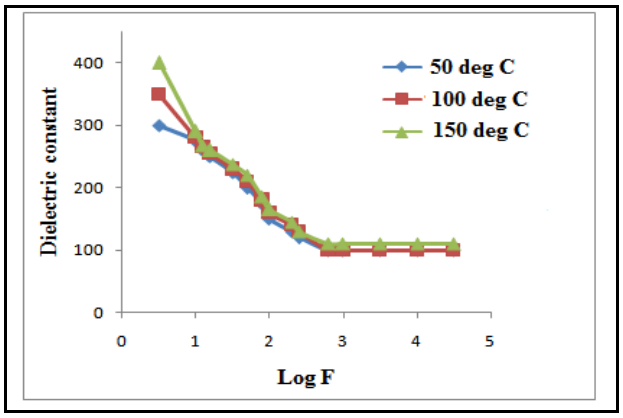

Fig. 13 Variation of dielectric loss with log f of LTCC crystal

3.8. Photoluminescence studies

Photoluminescence is measures of photo absorption in direct band gap material, from which the light emission of the material of a particular wavelength can be determined .To understand the luminescence property, photoluminescence (PL) spectrum of LTCC is recorded at room temperature with He–Ne laser of 20 mW input energy with the excitation wavelength 633 nm. The analysis of spectrum shown in Fig.14, gives a strong emission peak at 615 nm, which confirms that the spectrum of grown crystal emits green radiation under excitation [32]. This green band emission at 2.02 eV may be attributed to radioactive recombination between donars and acceptors that is the protonation of amino group to the carboxyl group [33]. Also, this charge transfer and protonation of charge is highly coherent with second order NLO activity, where the crystal emits green signal for photon absorption. However, the strong emission may indicate the presence of intrinsic defects in the forbidden band region.

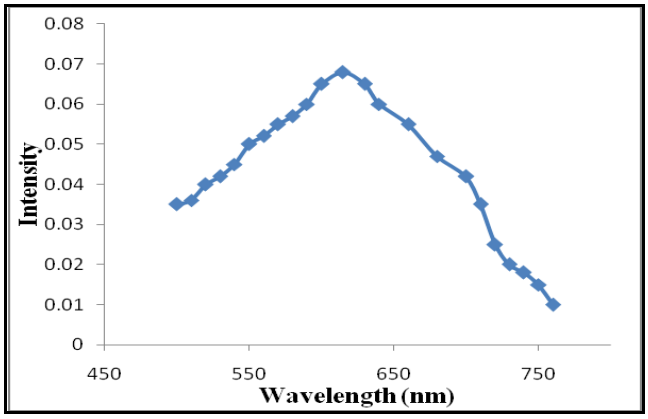

Fig.14 PL emission spectrum of LTCC crystal

3.9 Laser damage studies

Like other optical materials used in Laser technology, NLO crystals are susceptible to optically induced catastrophic damage. Optical damage in non-metals (dielectrics) may severely affect the performance of high power laser systems as well as the efficiency of optical systems based on nonlinear process and has therefore been subject to extensive research for some 30 years [34]. In this view, we carried out laser damage threshold measurements on LTCC crystal on (2 0 2) plane were determined using expending a Q-switched Nd:YAG laser (operating in TEM_{00} mode) of 20 ns laser pulses at a wavelength of 1064 nm. The schematic of experimental setup has been described earlier [35]. The laser beam divergence was 2.5 mrad. A variable attenuator was habituated to control the output intensity of the laser. A photodiode was used to identify the pulse-to-pulse variation of the laser beam. The output from the laser was rendered to the test sample ensconced at the near focus of the converging lens. The lens with a focal length of 5 cm was used, which facilitates in setting the spot size to the coveted value. The sample was mounted on the goniometer (to position the different sites in the beam) and kept slightly away from the focal spot of the beam. During laser irradiation, the power meter records the intensity of the input laser beam for which the crystal gets damaged. Single shot laser damage measurement was made on the polished face of the grown crystal, which is relevant for second harmonic generation. The occurrence of damage was monitored and irrespective of whether the damage had occurred, the sample was moved to a new site. The distance between the two sites was so kept 2–3 times the spot size on the crystal surface to avoid the possible cumulative effect that may reduce the actual damage resistance value of the crystal. The experiment was repeated for many samples of the same crystal, and the average was taken for calculations. The energy density was calculated as

$$D = \frac{E}{A}\left(\frac{GW}{cm^2}\right) \quad (16)$$

where D is the energy density, E is the input energy in milli joules and A is the area of the circular spot size. For the title crystal it was found to be 3.12 GW/cm^2. It is observed that the damage threshold of LTCC is many times higher than KDP (0.20 GW/cm^2). For multiple shot modes, the observed value is less compared to the above said value. It reveals the fact that single shot damage threshold is higher than the multiple shot damage. Apart from thermal effect, multi photon ionization is the important cause of laser induced damage. For pulse widths that stretch into several nanoseconds, thermal effects are unavoidable while for picosecond pulse widths, thermal effects are negligible. This could be reasoned out that the thermal effects take several nanoseconds to buildup and could take several milliseconds to decay.

3.10 Second harmonic generation (SHG) study

The nonlinear optical (NLO) property of the grown crystal was confirmed by Kurtz and Perry powder test [36]. The LTCC single crystal was powdered with uniform particle size and this powder was packed densely between two transparent glass slides. KDP crystal was powdered to the identical size and was used as reference material in the SHG measurement. The Nd:YAG laser beam of 1064 nm wavelength, 8 ns pulse with 10HZ pulse rate was made to fall on the sample .The second harmonic generation in the crystal is confirmed with the emission green light as output. For the constant input energy of 1.9 mJ/pulse supplied for both crystals the output power is found to be 9.2 mV for LAPP and 9 mV for KDP respectively. Hence the SHG efficiency of grown crystal was found to be 1.022 times greater than that of KDP. The result suggests that LTCC crystal can be used effectively to optical and photonic device applications.

Conclusions

Unidirectional crystal growth technique has been employed for the growth of semi organic L-threonine cadmium chloride (LTCC) single crystal along (2 0 2) plane, with high solute-crystal conversion efficiency. Single crystal XRD confirms that the crystal belongs to orthorhombic system with the space group $P2_12_12_1$. Powder X-ray diffraction reveals the perfect orientation crystallites and growth of the crystal along (2 0 2) plane. UV-VIS spectrum shows that the crystal possesses high transparency in the entire visible with a wide band gap of 3.75 eV.

Microhardness measurement reveals that Vickers' hardness number increases as the load increases and then decreases for higher loads, satisfying reverse indentation size effect. The low dielectric constant and dielectric loss at high frequencies suggest that the sample possesses enhanced optical quality with lesser defects. The photoluminescence spectrum shows a strong green emission indicating the high charge transfer for protonation. Kurtz powder test shows that the SHG sufficiency of LTCC is nearly 1.022 times of standard KDP

crystal. The laser damage threshold on the (2 0 2) plane of the LTCC is found to be 3.12 GW/cm^2 for a single shot mode. The detailed characterization and the nonlinear optical properties confirm that the grown crystal is suitable for the fabrication of various optoelectronic and photonic devices along the favorable orientation (2 0 2).

References

1. S.Chenthamarai, D.Jayaraman, P.M.Ushasree, K.Meera, C.Subramanian, P. Ramasamy, Mater.Chem. Phys.64 (2000)179-192.
2. M.S.Wong, C.Bosshard, F.Pan, P.Gunter, Adv.Mater.8 (1996)677.
3. V.G.Dmitriev, G.G.Gurzadyan, D.N.Nicogosyan, Hand book of Nonlinear Optical Crystals, Springer-Verlag, NewYork,1999.
4. Y.R.Shen, ThePrinciplesofNonlinearOptics, Wiley, NewYork,1984.
5. H.O.Marcy, L.F.Warren, M.S.Webb,C.A.Ebbers, S.P.Velsko,G.C.Kennedy, Appl. Opt.31 (1992)5051-5063.
6. S.Ledoux, J.Zyss,J.Int.,NonlinearOpt.Phys.3(1994)287-298.
7. D.Xu, M.Jiang, Z.Tan, ActaChem.Sin.41 (1983)570-579.
8. B.SureshKumar, M.R.SudarsanaKumar, K.RajendraBabu, Cryst.Res.Technol. 43(2008) 745-753.
9. D.Eimerl, S.Velsko, L.Davis, F.Wang, G.Loiacono, G.Kennedy, EEEJ.QuantumElectron.25 (1989)179–193.
10. S.Dhanuskodi, J.Ramajothi, Cryst.Res.Technol.39 (2004) 592–597.
11. K.Kirubavathi, K.Selvaraju, R.Valluvan, N.Vijayan, S.Kumararaman, Spectrochim.ActaA69 (2008) 1283–1286.
12. S.Dhanuskodi, K.Vasantha, P.A.AngeliMary,Spectrochim. Acta A66 (2007) 637–642.
13. M.Anbuchezhiyan, S.Ponnusamy, C.Muthamizhchelvan, K.Sivakumar,Res.Bull.45 (2010) 897-904
14. Redrothu Haumatharo,S.Kalainathan,Spectrochim.Acta A86 (2012) 80-84
15. S. Masilamani, A. Mohamed Musthafa, , Arabian Journal of Chemistry (2014) 134-149
16. P.M. Ushashree, R. Muralidharan, R. Jayavel, P. Ramasamy, J. Cryst. Growth 218 (2000) 365-371
17. K. Sankaranarayanan, P. Ramasamy, J. Cryst. Growth 280 (2005) 467-473.
18. S.Natarajan, K.Moovendhan, S.Mohanraju, K.Sethuraman, ,Optik 125(2014) 2505-2508
19. K. Sankaranarayanan, P. Ramasamy, J. Cryst. Growth 292 (2006) 445-448.
20. R. Uthrakumar , C. Vesta , C. Justin Raj , S. Krishnan , S. Jerome Das , Current Applied Physics 10 (2010) 548–552.
21. V. Venkataramanan, S. Maheswaran, J.N. Sherwood, H.L. Bhat, J. Cryst. Growth 179 (1997) 605-610.
22. C. Justin Raj, S. Jerome Das, J. Cryst. Growth 304 (2007) 191–195
23. V.Pandey, N.Mehta, S.K.Tripathi, A.Kumar, ChalcogenideLett.2 (2005)39-47.
24. M.Dongol, Egypt.J.Solids25 (2002)33-45.
25. B.L. Zhu, C.S. Xie, D.W. Zeng, W.L. Song, A.H. Wang, Mater. Chem. Phys. 89 (2005)148–153.
26. A. Ashour, N. El-Kadry, S.A. Mahmoud, Thin Solid Films 269 (1995) 117–120.
27. S. Krishnan, C. Justin Raj, S. Dinakaran, S. Jerome Das, Cryst. Res. Technol. 43(2008) 670–673.
28. B.W. Mott, Micro Indentation Hardness Testing, Butterworths, London (1956) p.9.
29. P. Mythili, T. Kanagasekaran, N. Shailesh, R. Sharma, Gopalakrishnan, J. Cryst. Growth 306 (2007) 344-350.
30. P.C. Thomas, S. Aruna, J. Packiam Julius, A. Joseph Arul Pragasam, P. Sagayaraj,Cryst. Res. Technol. 41 (2006) 1231–1235.
31. Christo Balarew, Rumen Duhlev, J. Solid State Chem. 55 (1) (1984) 1–6.
32. L. Guru Prasad, R. Nagalakshmi, P. Muthusamy , V. Krishnakumar, ,Materials Letters 63 (2009) 1255–1257..
33. Kanagasekaran T, Mythili P, Srinivasan P, Shailesh N, Sharma, Gopalakrishnan R.,Mater Lett 2008; 62:2486–2489.
34. Sonal. S. Gupte, Ranjit D. Pradhan, A. Marcano, Noureddine Melikechi, J. Appl. Phys. 91 (5) (2002) 3125-3138.
35. N. Vijayan, G. Bhagavannarayana, T. Kanagasekaran, R. Ramesh Babu, R. Gopalakrishnan, Ramasamy, Cryst. Res. Technol. 41 (8) (2006) 784-796.
36. S.K. Kurtz, T.T. Perry, J. Appl. Phys. 39 (1968) 3798-3813.

*****